Journal of Colloid and Interface Science 438 (2015) 159–168

Contents lists available at ScienceDirect

Journal of Colloid and Interface Science

www.elsevier.com/locate/jcis

Removal of strontium (Sr^{2+}) from aqueous solutions with titanosilicates obtained by the sol–gel method

Olga Oleksiienko [a,b,*], Irina Levchuk [b], Maciej Sitarz [c], Svitlana Meleshevych [a], Volodymyr Strelko [a], Mika Sillanpää [b]

[a] Institute of Sorption and Problems of Endoecology NAS of Ukraine, 13 General Naumov str., Kyiv 03164, Ukraine
[b] Laboratory of Green Chemistry, Lappeenranta University of Technology, Sammonkatu 12, Mikkeli 50130, Finland
[c] AGH University of Science and Technology, Faculty of Materials Science and Ceramics, Al. Mickiewicza 30, 30-059 Kraków, Poland

ARTICLE INFO

Article history:
Received 5 August 2014
Accepted 27 September 2014
Available online 8 October 2014

Keywords:
Titanosilicate
Sol–gel synthesis
Porous structure
Adsorption
Kinetic study

ABSTRACT

Titanosilicates (TiSis) were synthesized from pure and technical precursors by the sol–gel method. X-ray diffraction (XRD) studies of TiSi identified amorphous phases. The Brunauer, Emmett and Teller (BET) surface area of TiSis obtained from pure and technical precursors measured using the low-temperature nitrogen adsorption/desorption technique were 270.3 and 158.7 $m^2\ g^{-1}$, respectively. Micro-mesopore and micro- meso- macropore structures were attributed to TiSi prepared from pure and technical precursors, correspondingly. TiSis mass, solution pH, contact time, initial Sr^{2+} concentration, temperature and background solution were investigated for their effect on sorption properties. TiSis were observed to have a high affinity for strontium in the pH range of 4–12. Strontium adsorption isotherms were established and fitted to the Langmuir, Freundlich, Redlich–Peterson, Sips and Toth models. Pseudo-first and pseudo-second models were used to describe experimental kinetic data. X-ray photoelectron spectroscopy (XPS) and scanning electron microscopy with energy dispersive X-ray spectroscopy (SEM–EDX) data for TiSis were collected before and after adsorption. Heterophase was observed on the surfaces of both types of TiSi material after Sr^{2+} uptake. The mechanism of Sr^{2+} sorption on titanosilicates was suggested.

1. Introduction

Nuclear disasters such as Chernobyl and Fukushima lead to the release of radionuclides into the environment, which in turn has a harmful effect on all living organisms. This makes the removal of radionuclides from water and wastewater a key issue for today [1,2]. The development of new materials for contaminated wastewater treatment is thus attracting significant attention [3–7]. Titanosilicates are known as the most promising inorganic adsorbents for the decontamination of liquid radioactive wastes from long-lived radionuclides such as caesium and strontium. This can be explained by their high selectivity and stability over a wide pH range, high immutability with temperature variations and resistance to ionizing radiation [8,9]. Numerous studies of framework TiSis have reported on their various synthesis methods, structural and sorption properties [10,11]. Yet all known synthesis methods lead to titanosilicates in powder form only, which raises difficulties for their practical application. Granulated and particulate materials could be used in order to achieve a measure of success. One way of applying these kinds of material without any binders is by sol–gel method. Sol–gel synthesis has a number of benefits in comparison with conventional methods, such as synthesis at relatively low temperatures and the possibility synthesizing composite materials. These are difficult to achieve by traditional means due to the problems associated with volatilization, high melting temperatures or crystallization. Other important advantages of the sol–gel method are high purity and excellent homogeneity. This method can also be used to prepare a wide range of materials such as thin and thick films, fibres and bulk materials. Finally, sol–gel synthesis can obtain materials with the desired properties [12]. A novel approach to the sol–gel synthesis of titanosilicates was developed recently [13,14]. This method leads to the preparation of a stable gel with reproducible properties using simple inorganic salts, acids and alkali or alkaline earth hydroxides, and particles are then obtained by gel crushing. The influence of synthesis parameters on the crystal-chemical structure and adsorption capacity of the abovementioned materials have also been investigated [5,15,16]. The possibility to conduct a synthesis with technical precursors instead of pure chemicals was reported in [13,14]. It was found that a complexing cations (contained in technical precursor as a pollutants)

* Corresponding author at: Laboratory of Green Chemistry, Lappeenranta University of Technology, Sammonkatu 12, Mikkeli 50130, Finland.
E-mail address: ovalexis@gmail.com (O. Oleksiienko).

http://dx.doi.org/10.1016/j.jcis.2014.09.075
0021-9797/

affected the sol–gel processing. The present work seeks to investigate the influence of precursor substitution on the TiSi materials properties. Since obtained materials supposed to be used as adsorbents, the main attention of current study was paid to difference in sorption abilities and understanding the sorption mechanism on titanosilicates synthesized by sol–gel method with pure and technical precursors.

2. Experimental procedure

2.1. Chemicals

All chemicals used for analysis ($SrCl_2{\cdot}6H_2O$; NaCl, $NaHCO_3$, KCl, $CaCl_2$, D-glucose, H_2SO_4, HNO_3, HCl, NaOH) were of analytical grade (Sigma–Aldrich) and used without further purification. Technical liquid glass solution ($Na_2O{\cdot}2.5\ SiO_2$) and technical solution of $TiOSO_4$ were purchased from Ukrainian enterprises. Laboratory glassware was washed with concentrated HCl or HNO_3. Milli-Q water (resistance 18.2 M Ω cm) was used for all experiments.

2.2. Synthesis

Titanosilicates were prepared by sol–gel synthesis according to the scheme and procedure given in [13,14].

$$\text{inorganic salt Ti} + Na_2O \cdot SiO_2 + MOH \overset{HTT}{\rightarrow} \underset{gel}{M_xTi_ySi_zO_m \cdot nH_2O} \quad (1)$$

where HTT is hydrothermal treatment and MOH is alkali or alkaline earth hydroxides.

Pure and technical solutions of $TiOSO_4$ were used as an inorganic titanium salt and NaOH as MOH. Technical liquid glass solution was used as a source of silicon for titanosilicate synthesis.

Pure solution of $TiOSO_4$ was achieved by replacing Cl^- with SO_4^{2-} in $TiCl_4$. All chemicals used in this reaction were of analytical grade. A technical solution of $TiOSO_4$ was taken for synthesis after filtering through a polypropylene filter (0.5–1.0 mm). Pure or technical solutions of $TiOSO_4$, liquid glass and NaOH with the molar ratio Ti:Si:NaOH = 1:1:4 were used. TiSi gels were obtained at room temperature after magnetic stirring. The gels were then hydrothermally treated (HTT) in Teflon-lined steel autoclaves under autogenous pressure. The HTT gels were then rinsed with water and dried at 80 °C. Particles of prepared xerogel were ground, sieved and fractions with a size of 0.25–0.5 mm were used in the sorption studies.

2.3. Instrumentation

Measurements of pH were taken using a 340i pH-metre. The BET specific surface area, Barrett–Joyner–Halenda (BJH) and density functional theory (DFT) pore size distribution, DFT and Dubinin–Radushkevich (DR) micropore volume of TiSi were measured using a Quantachrome NOVA 2200 surface area analyser. The X-ray diffraction (XRD) patterns were recorded using DRON-4-07 (Cu Kα; 2θ = 5–80° step $\Delta 2\theta$ = 0.02°). An IKA KS 4000i control shaker–incubator was used for sorption tests at 200 rtp. The cation concentrations in solutions during sorption tests were investigated with an inductively coupled plasma optical atomic emission spectrometer (ICP–OES) model iCAP 6300 (Thermo Electron Corporation, USA). X-ray photoelectron spectroscopy (XPS) data were collected using a Thermo Fisher Scientific ESCALAB 250Xi. FTIR spectra were recorded with a Bruker Vertex 70v spectrometer. Spectra were collected in the mid (MIR) regions (4000–100 cm^{-1}) after 128 scans at 4 cm^{-1} resolution. Samples were prepared by the standard KBr pellets methods. Microstructure of the produced materials was examined by means of scanning electron microscope (SEM, Nova Nano SEM 200, FEI Company) with an attachment for chemical analysis of specimen in microareas with energy dispersive X-ray spectroscopy (EDX, EDAX). The experiment was carried out in low vacuum condition in secondary electron mode.

2.4. Adsorption experiments

Initial strontium solutions for the sorption experiments were prepared from solids of strontium chloride hexahydrate. Experiments were performed in batch tests using a shaker–incubator, and aqueous solutions of Sr^{2+} with different media such as water, NaCl and Ringer–Locke's (RL) solution. All batch tests were performed in polypropylene tubes. Polypropylene syringe membranes (0.45 μm) were used for sorbent separation. Adsorption capacity was investigated as a function of adsorbent mass, initial concentration, time, pH, temperature, composition and concentration of background solution. Control experiments (without sorbent material) were conducted at the same time with sorption experiment in order to illustrate, that sorption take place on the sorbent surface and not on the dish's surface.

The effect of ratio between adsorbent mass (m) and solution volume (V) on the adsorption capacity of TiSi was studied at V/m ratios from 50 to 2000. The initial concentration of Sr^{2+} was 0.5 g L^{-1}, the solution medium was 0.1 M NaCl and the pH was 7.08.

The influence of initial Sr^{2+} concentration on the sorption properties of TiSi was investigated in solutions with different media, such as water (pH = 6.78); NaCl at concentrations 0.01 M, 0.05 M, 0.1 M and 0.2 M (pH = 7.08) and Ringer–Locke's solution (9 g L^{-1} of NaCl, 0.2 g L^{-1} of $NaHCO_3$, 0.2 g L^{-1} of KCl, 0.2 g L^{-1} of $CaCl_2$ and 1 g L^{-1} of D–glucose; pH = 8.07). Initial strontium concentrations were varied from 10 to 5000 mg L^{-1}, the solution volume was 5 mL and the contact time was 24 h.

The effect of pH on the sorption properties of TiSi was evaluated from strontium solutions in water medium. Experiments were conducted at pH ranging from 1 to 12, with an initial Sr^{2+} concentration of 0.5 g L^{-1}, 5 mL solution volume and 24 h contact time.

The impact of contact time (t) on the adsorption capacity of TiSi was estimated using strontium solutions with water (pH = 6.78) and 0.1 M NaCl (pH = 7.08) media. The contact time ranged from 3 to 2880 min at ambient temperature (24 °C ± 2) and from 3 to 360 min at elevated temperatures. The initial Sr^{2+} concentration was 0.5 g L^{-1} and the solution volume was 5 mL.

The effect of temperature was studied with strontium solutions with 0.1 M NaCl (pH = 7.08 ± 0.02) as a medium. Sorption tests were conducted at temperatures of 40, 60 and 70 °C, at a contact time of 3–360 min, an initial Sr^{2+} concentration of 0.5 g L^{-1} and a solution volume of 10 mL.

Adsorption capacity (q), distribution coefficient (K_d) and decontamination factor (DF) were calculated using the following equations:

$$q = (C_o - C_t) \cdot \frac{V}{m} \quad (2)$$

$$K_d = \frac{(C_o - C_t)}{C_t} \cdot \frac{V}{m} \quad (3)$$

$$DF = (\Delta C \cdot 100\%)/C_0 \quad (4)$$

$$\Delta C = C_o - C_t$$

where C_o and C_t are initial concentration and concentration of strontium in solution (mmol L^{-1}) for time t, V is the aliquot volume (mL) and m is the mass of adsorbent (g).

Experimental data were fitted to the Langmuir, Freundlich, Sips (Langmuir–Freundlich), Redlich–Peterson and Toth models, which

are commonly used to describe liquid–solid systems [17–20]. The equations for these models are presented below:

$$q_e = \frac{q_m K_L C_e}{1 + K_L C_e} \quad (5)$$

$$q_e = K_F C_e^{1/n_F} \quad (6)$$

$$q_e = \frac{q_m (K_S C_e)^{n_S}}{1 + (K_S C_e)^{n_S}} \quad (7)$$

$$q_e = \frac{q_m K_{RP} C_e}{1 + (K_{RP} C_e)^{n_{RP}}} \quad (8)$$

$$q_e = \frac{q_m C_e}{(a_T + C_e^{m_T})^{\frac{1}{m_T}}} \quad (9)$$

where

q_e is the adsorption capacity (mg g^{-1} or mmol g^{-1}),
C_e is the equilibrium concentration,
K_L is the Langmuir sorption equilibrium constant (L mg^{-1} or L $mmol^{-1}$),
q_m is the maximum capacity (mg g^{-1} or mmol g^{-1}),
K_F is the Freundlich parameter in $mg^{1-1/n}$ $L^{1/n}$ g^{-1} ((mmol g^{-1})/(L $mmol^{-1}$)^{nF}),
n_F is the Freundlich parameter,
K_S is the affinity constant in (L $mmol^{-1}$),
n_S is the Sips parameter for surface heterogeneity description,
K_{RP} and n_{RP} are the Redlich–Peterson constants,
α_T is the adsorptive potential constant (mmol L^{-1}) and,
m_T is the Toth's heterogeneity factor.

The experimental kinetic data were fitted to the non-linear pseudo-first order model (PS1) and non-linear pseudo-second order model (PS2).

$$q_t = q_e^{-k_1 t} \quad (10)$$

$$q_t = \frac{k_2 q_e^2 t}{1 + k_2 q_e t} \quad (11)$$

where q_t and q_e are the adsorption capacity (mmol g^{-1}) at time t and at equilibrium respectively, while k_1 represents the PS1 rate constant (L min^{-1}), k_2 is the PS2 rate constant (g $mmol^{-1}$ min^{-1}) and $k_2 q_e^2$ represents the initial sorption rate.

The correlation between the experimental data and theoretical models was evaluated using the coefficient of determination (R^2). Calculations were carried out in Microsoft Excel.

$$R^2 = \frac{\sum (q_{e,exp} - \bar{q}_{e,exp})^2 - \sum (q_{e,exp} - q_{e,calc})^2}{\sum (q_{e,exp} - \bar{q}_{e,exp})^2} \quad (12)$$

where $q_{e,calc}$ is equilibrium capacity, calculated from the isotherm equation, $q_{e,exp}$ is equilibrium capacity obtained experimentally and $\bar{q}_{e,exp}$ is mean value of $q_{e,exp}$.

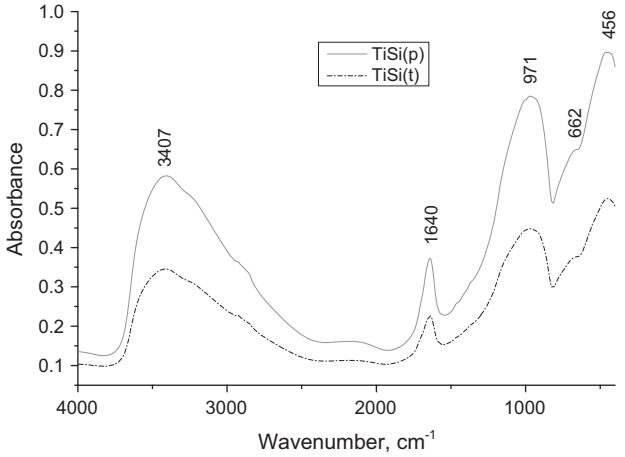

Fig. 1. MIR spectra of prepared TiSi materials.

3. Results and discussion

3.1. Characterization of the adsorbent materials

The titanosilicate materials prepared using chemically pure and technical solutions of titanyl sulphate ($TiOSO_4$) were characterized by XRD and FTIR. The X-ray patterns of the obtained materials were found to be amorphous (not shown). Fig. 1 presents a summary of the MIR spectra of output xerogels. On both spectra, two intense bands are shown at about 1640 and 3407–3327 cm^{-1} respectively. These bands are associated with stretching and bending vibrations of O–H bonds in the molecules of H_2O. An intense large band half-width is also shown at about 1110–800 cm^{-1} and 450 cm^{-1}. These bands are related to the presence of Si–O and Ti–O bonds. On TiSi xerogel spectra, the most characteristic feature is the presence of a band at 971–956 cm^{-1}, which is related to the presence of oxygen bridged Si–O–Ti bonds. In addition, however, a shoulder is also visible at about 1068 cm^{-1} which indicates the presence of Si–O–Si bonds. A very broad band with a maximum at about 450 cm^{-1} is related to the bending vibrations of O–Si–O and O–Ti–O bonds [21,22]. The morphology of the chosen samples was estimated by SEM (Fig. 2). As the images indicate the surfaces of both the technical and the pure samples are uneven and porous.

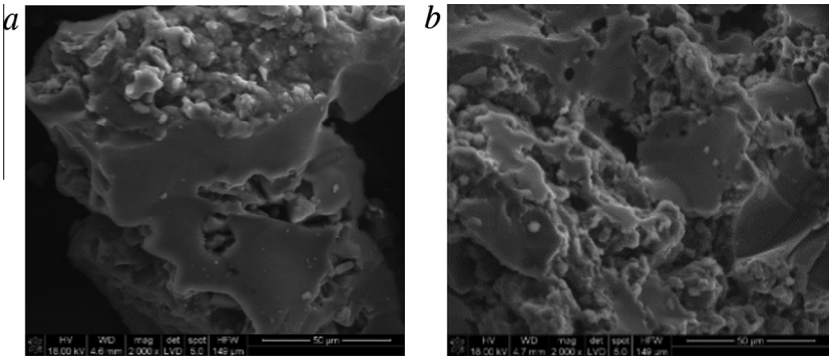

Fig. 2. SEM pictures of synthesized samples: (a) TiSi(p), and (b) TiSi(t).

The pore structure of the selected sorbents was defined by a low-temperature nitrogen adsorption/desorption technique. The isotherms and pore size distribution (DFT) are presented in Fig. 3. The titanosilicates produced are shown to have developed a porous structure. Type IV nitrogen adsorption isotherms with H2 hysteresis loops were derived from TiSi(p) IUPAC [23]. Isotherm and loop shape indicate the micro-mesopore structure of TiSi synthesized from a pure precursor. The H2 type of hysteresis loop suggests that the mesopores are ink-bottle shaped, with narrow necks and wide bodies. Type IV nitrogen adsorption isotherms with H1 hysteresis loops were derived from TiSi(t). The loops were narrow and not fully vertical over an appreciable range of N_2 uptake, suggesting a micro- meso- macropore structure for TiSi(t). It is probable that iron cations in the technical precursor promote the formation of a gel structure with minor differences between the mesopore necks and bodies. The pore size distribution verified the micro-mesopore structure of TiSi(p) and micro- meso- macropore structure of TiSi obtained from a technical precursor. The porous parameters were calculated using NOVAWin Surface Area Analyzer Quantachrome NOVA 2200 software. The results are presented in Table 1.

3.2. Adsorption experiments

In order to illustrate the effect of adsorbent mass on adsorption capacity, the ratio of adsorbent mass to aliquot volume is presented as a function of decontamination factor (DF). Decontamination factor was studied for ratios 50, 100, 200, 500, 1000, 2000 and 4000. Fig. 4 indicates that the maximum DF was observed at mass–volume ratio 100. Hence this value was used in subsequent adsorption investigations. It was worth to note that even at concentration of adsorbent 0.25 g L^{-1} (volume to mass ratio 4000) TiSis demonstrated high adsorption capacity to Sr^{2+} DF $\geqslant$ 90%.

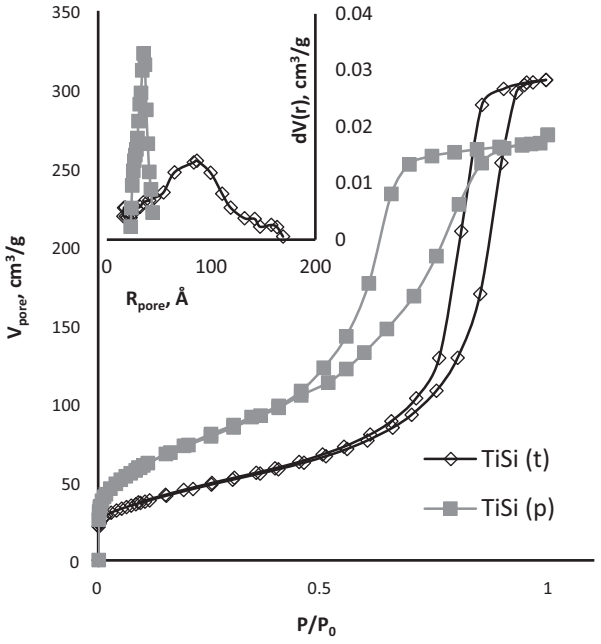

Fig. 3. Isotherms of nitrogen adsorption/desorption and pore size distribution of prepared titanosilicates.

Table 1
Structural properties of synthesized titanosilicates.

Sample name	S (m^2/g)	V_{total} (cm^3/g)	$V_{DR\ micro}$ (cm^3/g)	R_{pore} (nm)	$R_{micropore}$ (nm)
TiSi(t)	158.7	0.47	0.05	8.4	1.6
TiSi(p)	270.3	0.42	0.1	3.52	2.5

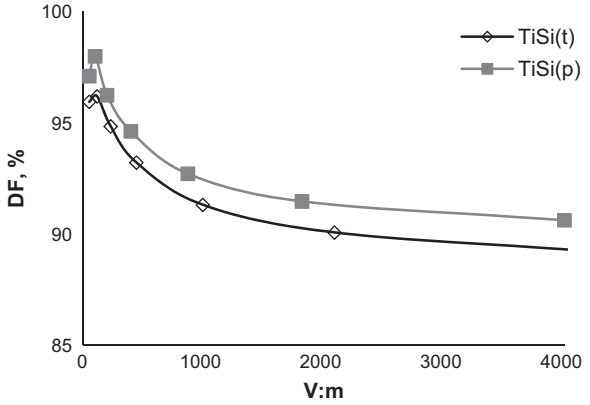

Fig. 4. Effect of volume to sorbent mass ratio on DF. Experimental conditions: initial concentrations of Sr^{2+} 0.5 g/l, background solution 0.1 M NaCl (pH = 7.08), ambient temperature.

The influence of initial strontium concentration on sorption properties was studied using solutions with different media in order to assess the impact of composition and concentration of background solution on titanosilicate ability to absorb Sr^{2+}. Data obtained with a water medium were used as a reference. High concentrations of sodium compounds in liquid radioactive wastes have been reported elsewhere [3,24], so the behavior of the material in the presence of these competitive ions was investigated. The simplest model solution, NaCl solution, was used to determine the competition effect of Na^+ and Sr^{2+} on the adsorption affinity of TiSi to Sr^{2+}. Ringer–Locke's solution was used to model both warm-blooded animal plasma [25] and seawater. A study of adsorbent affinity to Sr^{2+} in the presence of three competitive ions (Na^+, K^+, Ca^{2+}) was particularly interesting due to availability of these cations in seawater, blood plasma and drinking water. Concentrations of these cations are clearly lower in drinking water than in seawater, but it is possible to use the obtained data for predicting the sorption behavior of TiSi. As Fig. 5 shows, adsorption isotherms for different media have the H2 shape according to the Giles classification [26], which indicates the high affinity and selectivity to the adsorbate. It should be noted that background solution composition or concentration of competitive ions did not have any detectable effect on sorption capacity and the DF for both types of material was higher than 91% with initial strontium concentrations of up to 500 mg L^{-1}. Suppression of TiSi sorption capacity was observed in the presence of competitive ions at high initial strontium concentrations (1–5 g L^{-1}). Various reports indicate that sorption capacity of powder titanosilicate analogues (synthesised by precipitation method) decreases in the presence of high concentrations of competitive ions with much lower initial pollutant concentrations (10^{-9} = 10^{-3} M) [24,27,28].

A combination of stereochemical and physicochemical factors affect the selectivity of the adsorbent, including hydrated and ionic radius, hydration energy and complexing ability, valency and electrostatic interaction, cation mobility and space requirement. On the one hand Na^+ has smaller ionic radii and higher mobility compared to K^+, Ca^{2+} and Sr^{2+} and lower hydration energy than Ca^{2+} and Sr^{2+}. On the other hand, Sr^{2+} has higher valency and complexing ability than Na+, but also higher hydration energy [29–33]. Since the adsorption isotherms had the same shape in different background solutions, the Sr^{2+} sorption process was of greater energy benefit than that of Na^+, K^+ or Ca^{2+}.

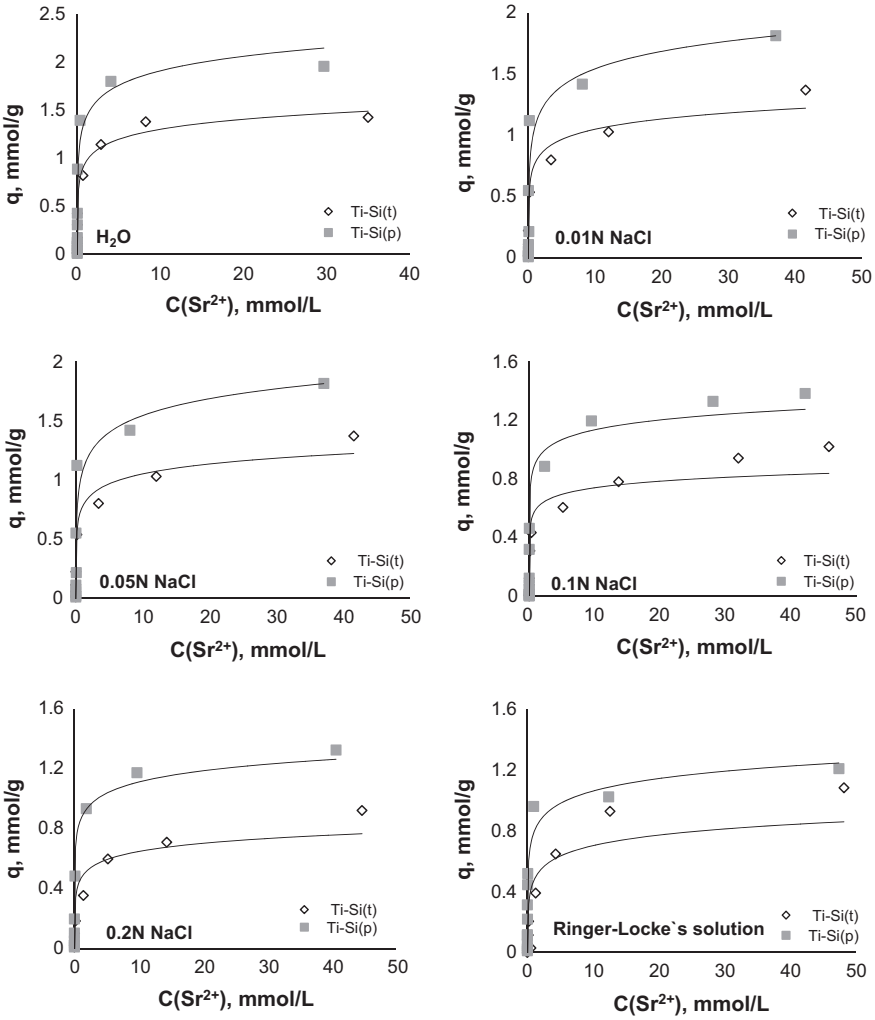

Fig. 5. Adsorption isotherms. Experimental conditions: initial strontium concentration range 10–5000 mg/l, solution volume 5 ml, contact time 24 h, media: water (pH = 6.78); 0.01 M, 0.05 M, 0.1 M, 0.2 M NaCl (pH = 7.08) and Ringer–Locke's solution (9 g L^{-1} of NaCl, 0.2 g L^{-1} of $NaHCO_3$, 0.2 g L^{-1} of KCl, 0.2 g L^{-1} of $CaCl_2$ and 1 g L^{-1} of D–glucose; pH = 8.07).

The maximum adsorption capacity of TiSi synthesized from pure precursors proved to be higher than that of TiSi obtained from technical precursors (Table 2). This could be ascribed to the lower specific surface of TiSi(t), resulting in a lower number of sorption active centres. Previous investigations with analogous materials synthesized by precipitation method with followed HTT [16] demonstrated that mesopores play a role in transporting small cations and that the sorption process mainly occurs in micropores. The micropore volume of TiSi samples declined steeply or was not available for N_2 and H_2O detecting molecules at all after adsorption tests [16]. Micropores and tunnels have been proposed as a sorption location for other crystalline TiSi ion-exchangers [10,34,35]. Thus reduction sorption also could be attributed to the lower micropore volume of TiSi synthesised from a technical precursor.

The sorption capacity of TiSi as a function of pH is presented in Fig. 6. The effect of pH ranging from 4 to 12 on the sorption properties of TiSi appears to be negligible. It is known that cation adsorption (cation exchange) increases with pH [28,36]. The high DF and low influence of pH illustrate the selectivity and chemical stability of the obtained amorphous materials. Below pH 4 sorption capacity suppression occurs, which can be explained by competition between Sr^{2+} and increased concentrations of anomalous mobile H^+ [28,36,37]. For example at pH 2 the DF for TiSi(p) declined by 10% and the DF of TiSi(t) by 27% compared to data at pH 4. An analogous effect has also been observed for powder titanosilicates [3,24].

The effect of contact time on the DF of Sr^{2+} was studied in time range 3–2880 min. The kinetic curves presented in Fig. 7 illustrate

Table 2
The maximum adsorption capacities of titanosilicate materials to Sr^{2+} at different background solutions.

q_{eq} (mmol/g)						
Background solution	H_2O	NaCl				Ringer–Locke's solution
		0.01 M	0.05 M	0.1 M	0.2 M	
Sample name						
TiSi(p)	1.95	1.81	1.40	1.38	1.32	1.21
TiSi(t)	1.42	1.37	1.13	1.02	0.92	1.08

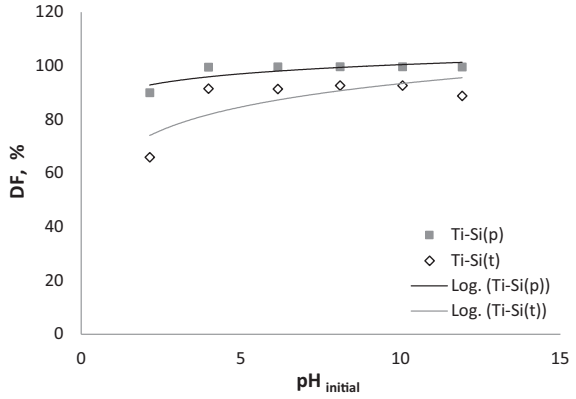

Fig. 6. Effect of pH on DF. Experimental conditions: pH from 2 to 12, Sr^{2+} initial concentration 0.5 g/l, solution volume 5 ml, contact time 24 h, ambient temperature.

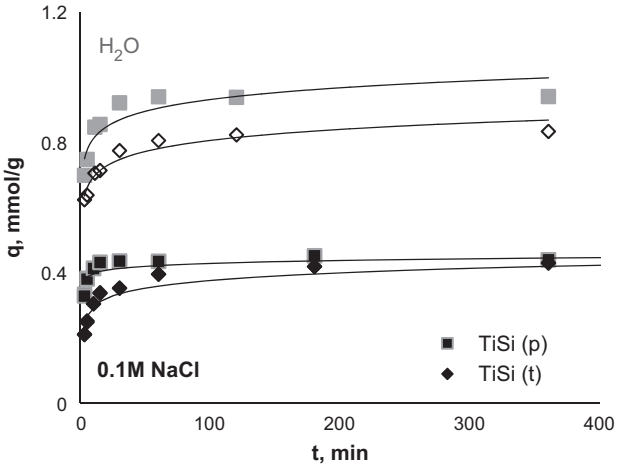

Fig. 7. Kinetics of Sr^{2+} sorption on titanosilicates. Experimental conditions: time range 3–2880 min, initial concentration of Sr^{2+} 0.5 g/l; solution volume 5 ml, background solutions – water (pH = 6.78) and 0.1 M NaCl (pH = 7.08), ambient temperature.

that both titanosilicate materials have the ability to remove Sr^{2+} from water at a relatively high rate. A DF of more than 70% was observed already after the first 3 min. Equilibrium was reached for TiSi(p) after a contact time of only 30 min while for TiSi(t) it took 60 min. The shape of the kinetic curves suggests that the sorption process could be separated into at least two steps: a high rate stage (the first 10–30 min) followed by a slow rate stage. The variation in Sr^{2+} uptake for different materials can be attributed to the microporous widths and micropore volume of these materials (Table 1). Consequently, TiSi(t) has smaller diameter and volume of micropores, which resulting in slower Sr^{2+} uptake.

A 0.1 M NaCl background illustrates the effect of Na^+/Sr^{2+} competition on the adsorption rate (Fig. 7). The medium impacted significantly: the presence of Na^+ decreases the uptake rate of TiSi(t) dramatically in the first 5 min. The initial parts of the kinetics curves became more vertical and the sorption capacity of both materials was suppressed. Nevertheless, both samples had reached equilibrium after the same length of time as in water. It was concluded that Na^+/Sr^{2+} competition affects titanosilicate sorption kinetics only during the high rate stage, i.e. in the first 10–30 min, while it does not have a significant impact on the slow rate stage.

Decontamination factor as a function of time at different temperatures is shown in Fig. 8. This figure indicates that sorption capacity and rate increase with increasing temperature. For instance, at 60 °C the DF was 91% after just 3 min of sorption. The graph showing $K_d(Sr^{2+})$ plotted against contact time illustrates that at elevated temperatures the sorption rate is higher on TiSi(p) than on TiSi(t), which could be attributed to the larger volume and width of micropores available in pure materials. The higher Sr^{2+} sorption rate and capacity at elevated temperatures illustrate the endothermic nature of sorption process on obtained TiSis and may suggest an activated sorption [38–41] mechanism. It is known that physisorption and ion exchange decrease with increasing temperature [42,43].

3.3. Reaction mechanism

In order to understand the mechanism of sorption on synthesized titanosilicates, the obtained experimental data were fitted to theoretical models. The samples were collected after adsorption tests and studied with SEM, XRD and XPS. The adsorption isotherm

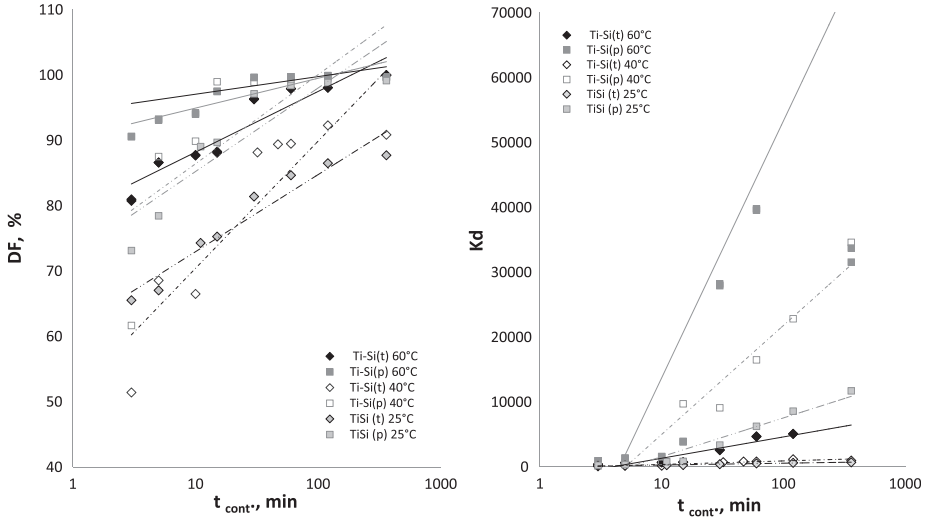

Fig. 8. Temperature effect on kinetics of Sr^{2+} sorption. Experimental conditions: contact time 3–360 min, Sr^{2+} initial concentration 0.5 g/l; solution volume 10 ml; adsorption temperature 25, 40 and 60 °C for medium 0.1 M NaCl (pH = 7.08).

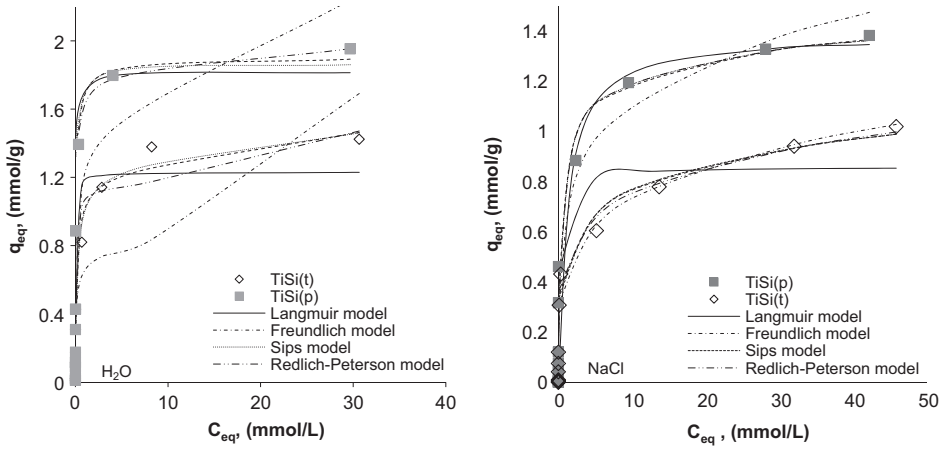

Fig. 9. Results of adsorption isotherm data modelling. Media: water and 0.1 M NaCl.

Table 3
Adsorption isotherm parameters obtained for synthesized TiSi.

Model	H_2O						0.01 M NaCl					
	TiSi(p)			TiSi(t)			TiSi(p)			TiSi(t)		
	q_{exp} (mmol/g)	$q_{calc.}$ (mmol/g)	R^2	q_{exp} (mmol/g)	$q_{calc.}$ (mmol/g)	R^2	q_{exp} (mmol/g)	$q_{calc.}$ (mmol/g)	R^2	q_{exp} (mmol/g)	$q_{calc.}$ (mmol/g)	R^2
Langmuir	1.95	1.81	0.981	1.42	1.23	0.938	1.38	1.35	0.917	1.02	0.85	0.943
Freundlich	1.95	2.24	0.837	1.42	1.69	0.709	1.38	1.48	0.971	1.02	1.03	0.987
Sips	1.95	1.86	0.982	1.42	1.46	0.978	1.38	1.36	0.987	1.02	0.99	0.990
Redlich–Peterson	1.95	1.98	0.990	1.42	1.47	0.967	1.38	1.40	0.998	1.02	1.0	0.996
Toth	1.95	1.89	0.985	1.42	1.46	0.979	1.38	1.37	0.992	1.02	0.99	0.993

data were fitted to the Langmuir, Freundlich, Sips, Redlich–Peterson and Toth models as shown in Fig. 9. This figure and Table 3 indicate that the Sips, Toth and Redlich–Peterson models, which consider surface heterogeneity assumptions and the possibility of interaction between the adsorbed substances, describe the experimental data better than the Langmuir and Freundlich models. The determination coefficient values were in the range of 0.967–0.996. The kinetic data were described using nonlinear pseudo-first order and pseudo-second order equations; the latter clearly described the data better ($R^2 \geqslant 0.993$; see Fig. 10 and Table 4). The pseudo-second order model assumes that the rate-limiting step is likely to be activated sorption or chemisorption involving valence forces, due to the exchange or sharing of electrons between the sorbent and sorbate [31,38,39,43].

The SEM images illustrate heterophase on the surfaces of both TiSi samples after sorption tests (Fig. 11). Acicular crystals in spherical aggregates measuring 2–5.5 μm were observed on both TiSi(p) and TiSi(t). Hexagonal crystals were 1–7 μm in size on TiSi(p) and 5–15 μm on TiSi(t). SEM–EDX mapping data showed the localization of more strontium at crystal regions than in any other area (Fig. 11). XPS data confirm the presence of strontium and carbon on both TiSi spectra after sorption tests (Fig. 12). Both crystal morphologies are typical for strontium carbonate [44–46]. The XRD pattern confirms the presence of the same strontianite mineral phase for both types of heterophase on the TiSi(p) sample after Sr^{2+} adsorption. At first this was attributed to epitaxial growth of $Sr_x(OH)_y(CO_3)_z$ on the alkalic sorbent surface during drying in air. Since no precipitation or changes in the Sr^{2+} concentration were detected during the control experiments and for initial tested solutions, it was concluded that strontium carbonate formation was possible only in the presence of TiSis for the studied Sr^{2+} concentrations and during the studied time. After the same tests for adsorption Cs^+ with Ca^{2+} cations and drying in air, however, no heterophase was detected. Therefore it was suggested that

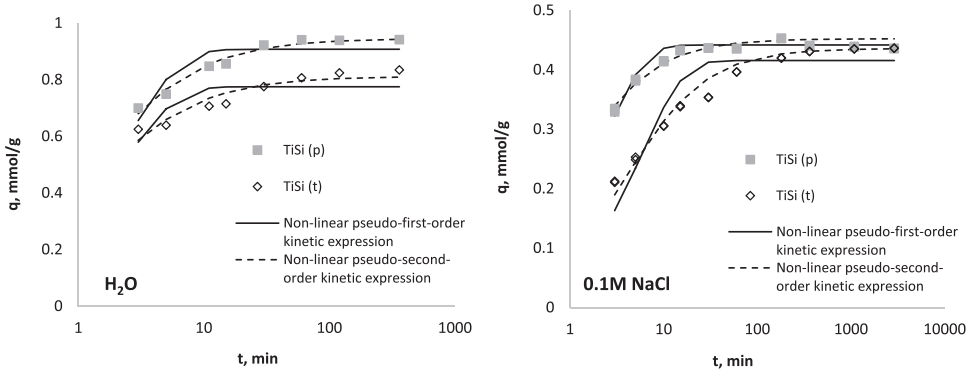

Fig. 10. Results of kinetic data modelling. Background solutions: water and 0.1 M NaCl.

Table 4
Kinetic parameters for strontium sorption on TiSi from 0.1 M NaCl.

Model	t, (°C)	TiSi(p)			TiSi(t)		
		$q_{exp.}$ (mmol/g)	$q_{calc.}$ (mmol/g)	R^2	$q_{exp.}$ (mmol/g)	$q_{calc.}$ (mmol/g)	R^2
Non-linear pseudo-first-order expression	25 [a]	0.941	0.907	0.784	0.835	0.775	0.575
	25	0.524	0.442	0.747	0.523	0.416	0.775
	40	0.950	0.956	0.862	0.864	0.852	0.932
	60	3.304	3.237	0.999	3.241	2.698	0.994
Non-linear pseudo-second-order expression	25 [a]	0.941	0.946	0.975	0.835	0.812	0.885
	25	0.524	0.452	0.802	0.523	0.436	0.919
	40	0.950	1.006	0.740	0.864	0.912	0.884
	60	3.304	3.291	1.0	3.241	2.698	0.993

[a] Adsorption from H_2O.

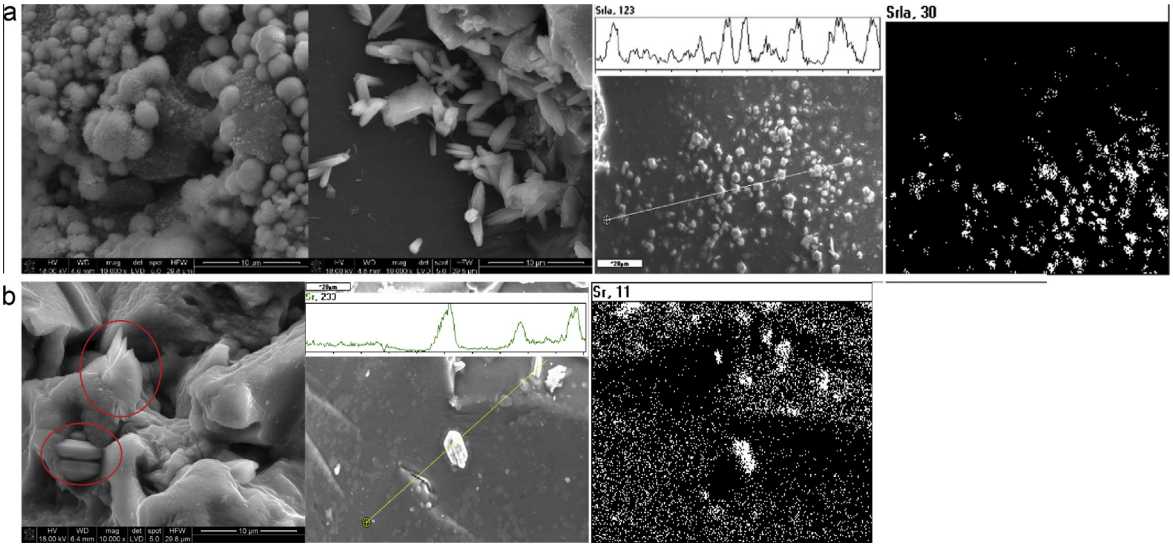

Fig. 11. SEM images with EDX of TiSis after Sr^{2+} adsorption: (a) TiSi(p), and (b) TiSi(t).

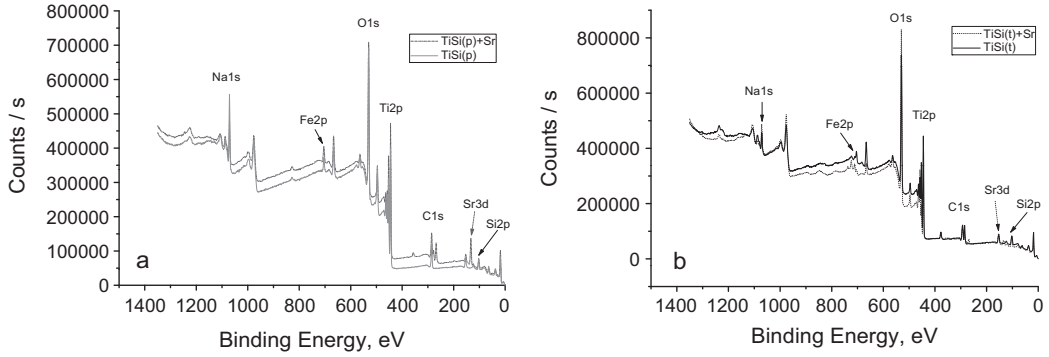

Fig. 12. XPS spectra of TiSi before and after sorption tests: (a) TiSi(p), and (b) TiSi(t).

one possible reason for Sr^{2+} selective sorption by TiSis could be participation of the CO_3^{2-}, $NaCO_3^-$ and HCO_3^- ions in the surface sorption process. Thus a hypothetical sorption mechanism was proposed.

Based on the FTIR results it was suggested that titanosilicate materials have the following surface ion-exchangeable groups: ≡Ti–O–Si–ONa, ≡Si–O–Ti–ONa and NaO–Si–O–Ti–ONa. It was entertained a possibility of the presence of the surface ion-exchange centres like ≡Si–O–Si–ONa and ≡Ti–O–Ti–ONa, but their role in titanosilicate adsorption capacity and selectivity was supposed negligibly. Based on literature data [9,35,47–49] it was assumed that the most active ion-exchange centres are ≡Ti–O–Si–ONa, ≡Si–O–Ti–ONa and NaO–Si–O–Ti–ONa.

The low dependence of TiSi sorption capacity on pH (pH ⩾ 4) and medium composition and concentration (up to 500 mg L^{-1} initial strontium concentration) suggests that Sr^{2+} sorption is dominated by inner sphere complexation [50]. It was reported elsewhere [29,30,33,40] that alkali and alkaline metals exchanged in dehydrated or partially dehydrated form. It follows from this assumption that cations reach the dehydration stage before the exchange. Dehydration is an endothermic process and its rate should increase with increasing temperature. This suggestion is in good agreement with

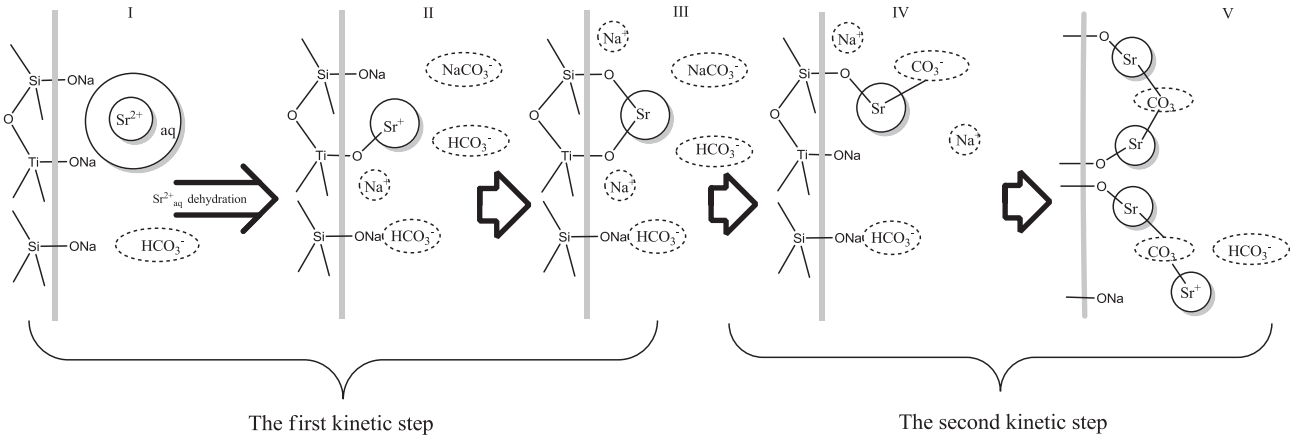

Fig. 13. Scheme of hypothetical sorption mechanism of Sr^{2+} on sol–gel prepared Titanosilicates.

the obtained kinetic data at elevated temperatures: sorption rates increased at the initial 'fast' parts of the kinetic curves.

During adsorption experiments pH rose by 2 ± 0.5, this was attributed to ion exchange between Sr^{2+} and Na^+. It is therefore proposed that the first step of the suggested mechanism is dehydration of hydrated strontium cation (Sr^{2+}_{aq}) near the exchange centre and ion exchange followed by inner sphere complexation. This step could represent the first kinetic stage with a high sorption rate while dehydration and/or inner sphere complexation could be the rate-limiting stages.

An interaction between the complexed by surface strontium and carbonate ions, which are usually present in aqueous solutions, was ascribed to the second step, at which the formation of strontium carbonate heterophase was observed. This step could represent the second part of the kinetic curve, with slow sorption rate and heterophase formation as a rate-limiting stage. This suggestion is in good agreement with the obtained sorption data at an elevated temperature: the rate and capacity of Sr^{2+} sorption were increased with increasing temperature. Fig. 13 presents a hypothetical scheme of the proposed mechanism. Additional studies of the sorption tests and sample drying in an inert atmosphere are needed, however, in order to confirm the proposed mechanism.

4. Conclusions

It was found that grade of precursor affected the pore structure of obtained titanosilicates, what reflected in different sorption capacity and uptake rate. TiSi prepared from a pure precursor had a higher adsorption capacity than material obtained from a technical precursor, estimated to be 1.95 mmol g^{-1} and 1.42 mmol g^{-1}, respectively. It was established that the Sr^{2+} uptake process on studied materials is rapid at ambient temperature and the rate increases at elevated temperatures. At room temperature the sorption process for both pure and technical TiSi follows pseudo-second order kinetic models. Scheme of possible Sr^{2+} sorption mechanism was proposed. The effect of competitive ions was investigated and no detectable effect on sorption capacity was observed for either type of material up to 500 mg L^{-1} initial strontium concentrations. Titanosilicates synthesized by the sol–gel method from pure and technical precursors proved to be highly efficient for strontium removal from aqueous solutions across a wide pH range. Obtained results lead to the conclusion that sol–gel synthesized TiSi can be effectively used for liquid radioactive wastewater decontamination instead of powder crystalline analogues TiSi [51,52]. Furthermore, it was suggested that proposed materials should be tested for blood plasma, mining, sea and drinking water purification from strontium.

Acknowledgments

The authors wish to thank Elisa Alasuvanto for her assistance with the sorption experiments. We are also grateful to Yurij M. Kylivnyk and Valerij I. Yakovlev for assisting with the precursor preparation and for our fruitful discussions. Furthermore, we thank Mukola M. Tsyba for supporting the porous investigations.

References

[1] H.N. Lee, in: S.E. Jørgensen, B.D. Fath (Eds.), Academic Press, Oxford, 2008. p. 2966.
[2] IAEA, IAEA, GC(57)/INF/3, 2013, 1.
[3] A.I. Bortun, L.N. Bortun, A. Clearfield, Solvent Extr. Ion Exch. 5 (1997) 909–929. http://dx.doi.org/10.1080/0736629970893451.
[4] A. Clearfield, Solvent Extr. Ion Exch. 18 (2000) 655. http://dx.doi.org/10.1080/073662900089347.
[5] F.J. Maringer, J. Šuráň, P. Kovář, B. Chauvenet, V. Peyres, E. García-Toraño, M.L. Cozzella, P. De Felice, B. Vodenik, M. Hult, U. Rosengård, M. Merimaa, L. Szücs, C. Jeffery, J.C.J. Dean, Z. Tymiński, D. Arnold, R. Hinca, G. Mirescu, Appl. Radiat. Isot. 81 (2013) 255. http://dx.doi.org/10.1016/j.apradiso.2013.03.046.
[6] N. Bolong, A.F. Ismail, M.R. Salim, T. Matsuura, Desalination 239 (2009) 229. http://dx.doi.org/10.1016/j.desal.2008.03.020.
[7] R.D. Ambashta, M.E.T. Sillanpää, J. Environ. Radioact. 105 (2012) 76. http://dx.doi.org/10.1016/j.jenvrad.2011.12.002.
[8] A. Clearfield, D.G. Medvedev, S. Kerlegon, T. Bosser, J.D. Burns, J. Milton, Solvent Extr. Ion Exch. 30 (2012) 229. http://dx.doi.org/10.1080/07366299.2011.639256.
[9] A. Tripathi, D.G. Medvedev, A. Clearfield, J. Solid State Chem. 178 (2005) 253. http://dx.doi.org/10.1016/j.jssc.2004.06.047.
[10] A. Clearfield, Solid State Sci. 3 (2001) 103. http://dx.doi.org/10.1016/S1293-2558(00)01113-4.
[11] J. Rocha, M.W. Anderson, Eur. J. Inorg. Chem. (2000) 801. doi:10.1002/(SICI)1099-0682(200005)2000:5<801::AID-EJIC801>3.0.CO;2-E.
[12] V.V. Strelko, J. Sol-Gel Sci. Technol. 68 (2013) 438. http://dx.doi.org/10.1007/s10971-013-2990-0.
[13] V.G. Kalenchuk, S.V. Meleshevych, V.A. Kanibolotsky, V.V. Strelko, O.V. Oleksienko, N.M. Patryliak, UA Patent 48457, 2010.
[14] V.V. Strelko, S.V. Meleshevych, V.A. Kanibolotsky, O.V. Oleksienko, UA Patent 66489, 2012.
[15] G. Lujaniene, S. Meleshevych, V. Kanibolotskyy, J. Sapolaite, V. Strelko, V. Remeikis, O. Oleksiienko, K. Ribokaite, T. Sciglo, J. Radioanal. Nucl. Chem. 282 (2009) 787. http://dx.doi.org/10.1007/s10967-009-0170-z.
[16] O.V. Oleksiienko, S.I. Meleshevych, V.V. Strelko, O.I. V'yunov, O.K. Matkovsky, V.G. Milgrandt, M.M. Tsyba, V.A. Kanibolotsky, Problems Chem. Chem. Technol. 2 (2013) 101.
[17] Y.S. Ho, J.F. Porter, G. McKay, Water Air Soil Poll. 141 (2002) 1.
[18] H.M.F. Freundlich, Z. Phys. Chem. 57A (1906) 358.
[19] Y. Liu, Y. Liu, Sep. Purif. Technol. 61 (2008) 229. http://dx.doi.org/10.1016/j.seppur.2007.10.002.
[20] K.Y. Foo, B.H. Hameed, Chem. Eng. J. 156 (2010) 2. http://dx.doi.org/10.1016/j.cej.2009.09.013.
[21] A.K. Brisdon, Inorganic Spectroscopic Methods, Oxford University Press, Oxford, 1998.
[22] K. Nakamoto, Infrared and Raman Spectra of Inorganic and Coordination Compounds, fifth ed., vol. A, Wiley-Interscience, New Jersey, U.S.A., 1997.
[23] K.S.W. Sing, Pure Appl. Chem. (1982) 2201. http://dx.doi.org/10.1351/pac198254112201.

[24] T. Möller, R. Harjula, J. Lehto, Sep. Purif. Technol. 28 (2002) 13. http://dx.doi.org/10.1016/S1383-5866(02)00004-7.
[25] L. Sehulster, R.Y.W. Chinn, MMWR 52 (RR10) (2003) 1.
[26] C.H. Giles, R.B. Mackay, J. Bacteriol. 89 (1965) 390.
[27] A. Clearfield, L.N. Bortun, A.I. Bortun, React. Funct. Polym. 43 (2000) 85. http://dx.doi.org/10.1016/S1381-5148(99)00005-X.
[28] A. Dyer, J. Newton, L. O'Brien, S. Owens, Microporous Mesoporous Mater. 120 (2009) 272. http://dx.doi.org/10.1016/j.micromeso.2008.11.016.
[29] I.M. El-Naggar, E.A. Mowafy, E.A. Abdel-Galil, Colloids Surf Physicochem. Eng. Aspects. 307 (2007) 77. http://dx.doi.org/10.1016/j.colsurfa.2007.05.004.
[30] J. Lehto, R. Harjula, Radiochim. Acta 86 (1999) 65. http://dx.doi.org/10.1524/ract.1999.86.12.65.
[31] I.M. Ali, E.S. Zakaria, H.F. Aly, J. Radioanal. Nucl. Chem. 285 (2010) 483. http://dx.doi.org/10.1007/s10967-010-0612-7.
[32] J. Burgess, Metal Ions in Solutions, Ellis Horwood, Chichester, England, 1978.
[33] I.M. El-Naggar, E.A. Mowafy, I.M. Ali, H.F. Aly, Adsorption 8 (2002) 225. http://dx.doi.org/10.1023/A:1021212617839.
[34] P. Sylvester, E.A. Behrens, G.M. Granziano, A. Clearfield, Sep. Sci. Technol. 34 (1999) 1981. http://dx.doi.org/10.1081/SS-100100750.
[35] E.A. Behrens, D.M. Poojary, A. Clearfield, Chem. Mater. 8 (1996) 1236. http://dx.doi.org/10.1021/cm950534c.
[36] A. Dyer, J. Newton, L. O'Brien, S. Owens, Microporous Mesoporous Mater. 117 (2009) 304. http://dx.doi.org/10.1016/j.micromeso.2008.07.003.
[37] A. Gierer, K. Wirtz, J. Chem. Phys. 17 (1949) 745. http://dx.doi.org/10.1063/1.1747388.
[38] T. Wolkenstein, Uspehi Fizicheskih Nauk. 2 (1953) 253.
[39] T. Wolkenstein, Electronic Processes on Semiconductor Surfaces during Chemisorption, Bureau, New York, 1991.
[40] W.G. Pollard, Phys. Rev. 56 (1939) 324. http://dx.doi.org/10.1103/PhysRev.56.324.
[41] L.E. Katz, L.J. Criscenti, C. Chen, J.P. Larentzos, H.M. Liljestrand, J. Colloid Interface Sci. 399 (2013) 68. http://dx.doi.org/10.1016/j.jcis.2012.05.011.
[42] W. Zuo, P. Han, Y. Li, X. Liu, X. He, R. Han, Water Treat. 12 (2009) 210. http://dx.doi.org/10.5004/dwt.2009.935.
[43] Y.S. Ho, G. McKay, Process Biochem. 34 (1999) 451. http://dx.doi.org/10.1016/S0032-9592(98)00112-5.
[44] M.A. Alavi, A. Morsali, Ultrason Sonochem. 17 (2010) 132. http://dx.doi.org/10.1016/j.ultsonch.2009.05.004.
[45] L. Li, R. Lin, Z. Tong, Q. Feng, Nanoscale Res. Lett. 7 (2012). http://dx.doi.org/10.1186/1556-276X-7-305.
[46] G. Guo, G. Yan, L. Wang, J. Huang, Mater Lett. 62 (2008) 4018. http://dx.doi.org/10.1016/j.matlet.2008.05.052.
[47] A. Tripathi, D.G. Medvedev, M. Nyman, A. Clearfield, J. Solid State Chem. 175 (2003). http://dx.doi.org/10.1016/S0022-4596(03)00145-2.
[48] D.M. Poojary, R.A. Cahill, A. Clearfield, Chem. Mater. 6 (1994) 2364. http://dx.doi.org/10.1021/cm00048a024.
[49] R.P. Nikolova, B.L. Shivachev, S. Ferdov, Microporous Mesoporous Mater. 165 (2013) 121. http://dx.doi.org/10.1016/j.micromeso.2012.07.053.
[50] W. Stumm, Chemistry of the Solid-Water Interface Processes at the Mineral-Water and Particle-Water Interface in Natural Systems, Wiley, New York, 1992.
[51] K. Popa, C.C. Pavel, Desalination 293 (2012) 78. http://dx.doi.org/10.1016/j.desal.2012.02.027.
[52] J.E. Miller, N.E. Brown, Sandia National Laboratories, SAND97-0771 l UC-721, UC-510, 1997.